Nigerian Research Journal of Engineering and Environmental Sciences 9(2) 2024 pp. 764-777
p ISSN: 2635-3342; e ISSN: 2635-3350

Nigerian Research Journal of Engineering and Environmental Sciences
Journal homepage: www.rjees.com

Original Research Article

Impact of Varying Austempering Treatment Parameters on Mechanical and Wear Properties of Austempered Ductile Iron

***Ochulor, E.F., Adeosun, S.O. and Awe, D.E.**

Department of Metallurgical and Materials Engineering, Faculty of Engineering, University of Lagos, Akoka, Lagos, Nigeria.
*eochulor@unilag.edu.ng

http://doi.org/10.5281/zenodo.14566187

ARTICLE INFORMATION

Article history:
Received 04 Nov. 2024
Revised 03 Dec. 2024
Accepted 05 Dec. 2024
Available online 30 Dec. 2024

Keywords:
Austempering temperature
Austempering time
Microstructure
Ausferrite phase
Retained austenite
Properties

ABSTRACT

Austempering temperature and time play an important role in the austempering mechanism and microstructural evolution of the l austempered ductile iron (ADI) part. In this study, as cast ductile iron (DI) samples were subjected to austempering treatment by adopting varying austempering temperatures of 300 °C, 350 °C and 400 °C and times of 20, 40 and 60 minutes. Samples were subjected to microstructural analysis via optical microscopy (OM) and Scanning electron microscopy (SEM), mechanical property testing, wear and X ray diffraction (XRD) analysis. Austempered samples consisted of needlelike and feathery ausferrite phase. The highest and lowest ultimate tensile test (UTS) values observed were 740 MPa at 300 °C for 20 minutes and 538 MPa at 400 °C for 60 minutes respectively. The UTS and vickers hardness of all austempered samples were higher than that of as cast sample's value of 480.3 MPa and 380 Hv respectively. Highest percent elongation of 7.7% was observed using 400°C for 60 minutes. The austempered samples had lower wear rates than their as cast counterpart. XRD patterns revealed growth of the ausferrite phase as austempering temperature increased. This study has established that there exists a crucial interplay between austempering temperature and time during austempering process.

1. INTRODUCTION

Ductile irons (DIs) also known as spheroidal cast irons (SCIs) or nodular cast irons (NCIs) are a type of cast irons which contain graphite in the nodular or spheroidal shape viz-a-viz the graphite flakes in gray cast irons (GCIs). The excellent properties of DI are mainly due to its microstructure which can be modified by adding alloying elements or by heat treatment (Olivera *et al.*, 2006). Austempered ductile irons (ADIs) are DIs which have been subjected to austempering heat treatment process which is an

isothermal heat treatment process. The DIs used for the austempering heat treatment must have the adequate chemical composition. ADIs have attractive mechanical properties as compared to conventional cast irons, steel castings, steel forgings and aluminum alloys (Vidyarthee and Singh, 2014; Bialobrzeski and Pezda, 2014; Mandal and Maity, 2013). The heat treatment methods could be the single step (conventional) and the dual step austempering processes (Wang *et al.,* 2020a). During this heat treatment there exists an interplay between the heat treatment parameters: austempering times and temperatures, which significantly impacts on phase transformation phenomenon, microstructure evolution, mechanical and wear properties of the product.

The properties of ADI are due to its unique matrix of acicular ferrite (α) and carbon-stabilized austenite (γ_{HC}) called Ausferrite, austenite in ADI has been stabilized with carbon during heat treatment and will not transform to brittle martensite. The combination of competitive mechanical properties makes ADIs one of the preferred materials for manufacturing components for commercial vehicles such as connecting rods, camshafts, crankshafts, transmission gears, and engine valves (Wang *et al.,* 2020a). ADIs are also used in wear applications such as rock drills and mining vehicles, during their service life these components are subjected to repeated surface contact with relative motion and external cyclic loads. This results in severe wear and fatigue damage; these combined effect leads to failure of the components. Thus, to ensure components with properties to meet the accepted service application and life, the component must have a high wear resistance and excellent fatigue strength (Mussa *et al.,* 2022). ADIs have found successful applications in many industries, including Construction and Mining, Agriculture, Automotive, Heavy Truck, and Railroad. ADI is almost 10% lighter than steel, and its superior capacity to absorb vibration and reduce noise from gearboxes (Magalhães *et al*., 2012).

The higher hardness grades of ADI have excellent wear characteristics, unlike case hardened materials, typically the ADI is uniformly hardened throughout the part. This property make ADIs are good choice for producing different gear types namely spur gears, helical gears, gear racks, bevel gears, and worms (Rajan *et al.,* 2011). Austempering heat treatment was generally done by heating the sample above the austenitizing temperature and holding it in that temperature range for sufficient time. The specimen is then quenched in salt bath medium kept at the austempering temperature and holding it for adequate time for the isothermal transformation, after which it is further cooled in air to room temperature.

Several studies have been conducted in literature to investigate the wear characteristics of the ADIs (Chiniforush *et al.,* 2016; Šolić *et al.*, 2016; Wang *et al*., 2020a; Wang *et al*., 2020b). These studies have reported that the wear performance of ADIs is influenced by the presence of graphite nodules in the matrix as well as the presence of carbon-rich austenite phase. In the study conducted in Krawiec *et al.* (2023), the researchers investigated the influence of heat treatment parameters of ADI on its microstructure, corrosion and tribological properties. They observed that a low value of the scratch depth, a high hardness at low values of the austempering temperature and short isothermal annealing time is related to the presence of martensite. The researchers concluded that increasing the isothermal annealing time from 30 to 120 minutes caused an increase in the fraction of ausferrite structures in relation to martensite. Also increasing the austempering temperature from 280 ^{o}C to 430 ^{o}C increased the transformation kinetics and, at the same time, affects the morphology of the final ausferrite structure. In Hegde and Sharma (2018), study on modified austempering process on manganese alloyed DI which involved multi-stage austempering heat treatments was conducted. The addition of manganese was done to improve the hardenability of the DI samples. The study concluded that, modified austempering process at 420 °C with 0.6 wt.% Mn compared with the conventional process improved hardness and UTS by 30 % and 40 %, respectively without compromising toughness. The researchers in Upkar and Rone (2019) conducted a review on the effect of copper on austempering behavior of DI, they concluded that as austempering temperature is increased the hardness and tensile strength are decreased and elongation is increased in both the copper alloyed DI and unalloyed DI. Also, as the austempering time is increases, the tensile strength, hardness and elongation are increased in both the grades adopted.

Some modifications have been made in the austempering process in the past few decades in other to improve the abrasion wear resistance of ADI, for example the introduction of a two-step austempering

which improved both mechanical properties and wear resistance through microstructural refinement (Yang and Putatunda 2005). Also, in Zhou *et al.* (2001), the researchers induced quenched martensite and retained austenite into the ausferrite matrix, this improved the impact abrasion resistance of the material. In the study conducted in Laino *et al.* (2008) chromium alloyed massive carbides was introduced into the microstructure of ADI, this enhanced wear resistance with compromise of impact toughness.

In many of these studies, the researchers investigated the effects of chemical composition and austempering parameters on microstructure and mechanical properties without investigating the wear properties of the heat treated ADIs. The wear performance of ADIs was discussed in Wang *et al.* (2020a), however being a review article, no heat treatment experiments were conducted, also most of the discussions were not based on the conventional austempering process which is a single step process but on the non-conventional one which is a dual step process. Based on these gaps discovered in literature, this study will investigate the effects of varying austempering temperature and time on evolved microstructure, mechanical and wear properties of the ADI samples to determine their interplay in the conventional austempering heat treatment process.

2. MATERIALS AND METHODS

2.1. Material Collection and Preparation of Samples

The materials adopted were silica sand, bentonite clay, steel scrap, DI returns, ferrosilicon alloy, ferrosilicon magnesium alloy and graphite coke to produce DI samples were sourced from Machine Tools Limited Osogbo. The mould was produced according to the requirements as outlined in ASTM E2349 standard mould making procedures, the moulding sand consisted of silica sand, bentonite, additives (coal dust and starch) and water. Consumables for metallography such as bakelite, alumina, diamond paste, silicon carbide powder and polishing papers were sourced from Metallurgical and Materials Engineering Department University of Lagos, Akoka. Lagos. The chemical composition of the graphite coke, ferro silicon alloy (FeSi) inoculant and ferro silicon magnesium alloy (FeSiMg) adopted for casting the DI samples are shown Tables 1, 2 and 3.

Table 1: Chemical composition of graphite coke

Element	C	Ash	S	Volatile matter	Moisture
Wt. %	72	27.5	0.2	<0.3	0.1

Table 2: Chemical composition of FeSi

Element	Si	Al	C	S	P	Fe
Wt. %	70	0.31	0.0032	0.001	0.001	29.68

Table 3: Chemical composition of FeSiMg

Element	Si	Mg	C	Fe
Wt. %	44.3	5.7	0.0032	29.68

The pattern used was a Y- block of ASTM A-536 specification for test coupons. Six mould boxes were prepared with the Y block cavity, the dimension of the Y block and the Y block pattern is shown in Figures 1a and 1b respectively. Melting was carried out in a 2000 kg dual track Induction furnace of model 13690/1954 inductotherm in Nigeria Machine Tools Osogbo, the charge materials consisted of steel scraps, DI returns, ferrosilicon and graphite, tapping was done at 1480 ^{o}C, 50kg of the melt was poured into the preheated treatment ladle. Nodularization treatment was performed via the sandwich process using FeSiMg alloy granules covered with mild steel chips in the treatment ladle. Two stage inoculation treatment was done for optimum graphite precipitation, firstly the FeSi inoculants were added to the melt in the pouring ladle after transfer from the treatment ladle. Further inoculation was also carried out while pouring into the moulds using a perforated pipe that delivered powdered

ferrosilicon into the melt stream. The moulds were then left to cool after pouring, fettling was later done to isolate blocks.

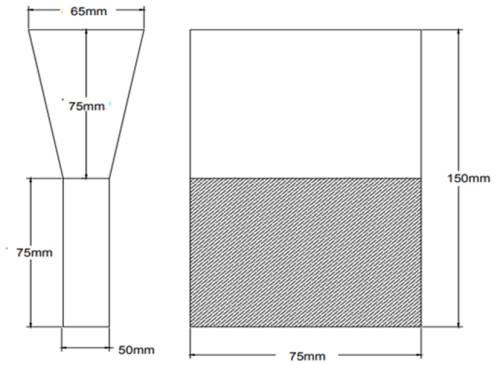

Figure 1a: Y-block Dimensions Figure 1b: Y-block pattern

2.2. Austenization Treatment

The cast DI samples were machined to tensile, hardness, microstructure and wear rate test sizes. A Carbolite Muffle Heat Treatment Furnace serial No 7/99/1635 type RHF 16/3 was adopted for the austenizing treatment. The samples were first austenized to 910 ^{o}C for twenty-four (24) minutes after which three austempering temperatures and three austempering (soaking) times for each temperature was adopted.

2.3. Austempering Heat Treatment

The austempering salt bath for the austempering treatment consisted of sodium nitrate ($NaNO_3$) and potassium nitrate (KNO_3) of the ratio 1:1. The sample designations for each austempering time and temperature are shown in Table 4. The austempering salt was placed in a porcelain crucible in another furnace and heated to 400 ^{o}C, and the heat maintained at 400 ^{o}C. The A samples for austempering were then treated by quenching them in the salt bath at 400 ^{o}C and held isothermally for varying soaking times of 20 minutes, 40 minutes and 60 minutes after which they were air cooled to room temperature. The procedure was repeated for 350 ^{o}C and 300 ^{o}C austempering temperatures with the same austempering times.

Table 4: Sample designation with austempering times and temperature

S/N	Sample designation	Holding time in salt bath in minutes (Austempering time)	Austempering temperature (^{o}C)
1	A1	20	
2	A2	40	300
3	A3	60	
4	B1	20	
5	B2	40	350
6	B3	60	
7	C1	20	
8	C2	40	400
9	C3	60	

2.4. Microstructural Characterization of DI and ADI samples

The samples were prepared according to specifications outlined in ASTM E3-11 standard for metallographic specimen. Samples were sectioned and mounted using a semi-automatic Buehler hot mounting press. The thermosetting bakelite was poured into the cylinder, locked and heated up to 200 ^{o}C. Grinding was done using LECO BG20 grinder using SiC abrasive papers, whereas polishing

operation was done on a mechanized polishing wheel using a sylvelte cloth and successive alumina (Al_2O_3) polishing paste 5µm, 1µm, 0.5µm and 0.05µm for final polishing.

Etching was done using 2% Nital (2ml nitric acid in 98ml ethanol), samples were dried and ready for microscopy. Microstructural characterization was carried out using CETI Optical Metallurgical Microscope (model no 0703552) located at the Metallurgical and Materials Engineering Laboratory, University of Lagos and scanning electron microscope model JEOL JSM-5900LV equipped with energy dispersive X-ray spectroscope (EDS).

2.5. Tensile Test

Tensile tests were done according to specifications outlined in ASTM E8/E8M standard (ASTM 2022) using a computer controlled 100 kN capacity Universal Instron Machine model 3369 at a constant cross head speed of 1mm/min at room temperature. The yield and ultimate tensile stress were determined as well as the elongation from the computer software as a graph of stress/strain is plotted, this was done for all the samples: for the control DI samples and all the austempered samples. The schematic drawing of the tensile test sample is shown in Figure 2.

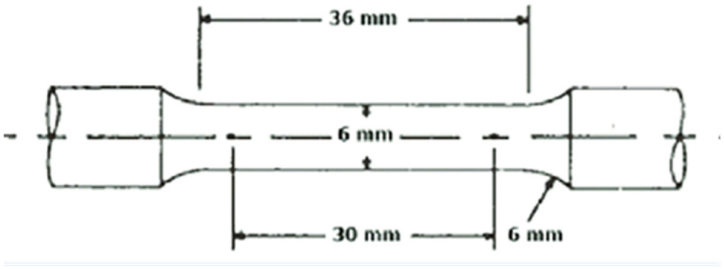

Figure 2: Dimension of tensile test piece

2.6. Hardness Test

Hardness test was carried out using Vickers micro hardness tester was done in accordance with ASTM E384-11 standard. The sample surface was first polished for smoothness using a polishing wheel, then placed on the tester, the indenter was allowed to press on the surface for about 10 seconds. After indentation, the resulting indent was analysed optically to measure the length of diagonals and determine the size of the impression.

2.7. Wear Test

The samples for the wear tests were in the form of 4 mm pins which were prepared in a lathe machine and then subjected to abrasive wear test conducted on a pin-on disk machine according to specifications outlined in ASTM G99. A hardened circular steel disk with hardness of 64 HRC was used as counter face. The machined test samples were placed into the tester allowing the sample to rub against the hardened revolving disk for a given normal load and speed condition. The disk was allowed to rotate for a predetermined period at a varying sliding moment for 60 seconds. The specimens were taken out at regular intervals and the weight was recorded. This procedure was repeated for all the samples after which the weight of the worn surfaces was obtained as the volume loss/wear volume in mm3 which was then used to determine the wear rate.

2.8. X-ray Diffraction (XRD) of samples

X-ray Diffractometer (XRD) Thermo scientific model: ARL'XTRA X-ray and serial number 197492086 at Engineering Laboratory, Musa Yar'dua University Kaduna was adopted for the analysis, the intensity of the peaks was used to determine the phases present in the samples. The intensity of diffracted X-rays is continuously recorded as the sample and detector rotate through their respective angles. The samples were polished to ensure smooth and defect free surface, they were then subjected

to XRD analysis using chromium Kα radiation. Scanning was done in the 2θ range of 10-80° to get the austenite and ferrite peaks.

3. RESULTS AND DISCUSSION

The chemical composition of the cast DI sample is shown in Table 5. All the elements in the cast DI sample are within the range accepted for DI, and to enhance austemperability of the as cast DI sample.

Table 5: Chemical composition of cast ductile iron

Element	C	Si	Mg	Mn	Cu	Ni	Cr	Fe
Wt. %	3.27	2.79	0.04	0.32	0.39	0.44	0.06	92.68

3.1. Optical Micrographs of Cast DI and ADI Samples

The as-cast microstructure of DI samples (etched in 4% nital) used for the austempering heat treatment is shown in Figure 3. This microstructure consists mainly of graphite nodules between 10-20 microns in size embedded in a matrix comprising of the ferrite and then surrounded by pearlite phase, typically known as the "bull eyes structure". In the ADI samples the morphology of acicular ferrite, carbon enriched austenite and retained austenite are strongly dependent on the austempering temperature and austempering time. For samples austempered at 300 ^{o}C, the microstructure consisted of a mixture of ausferrite i.e. acicular ferrite in carbon saturated austenite, untransformed austenite called retained austenite and graphite nodules, this microstructure was also observed in Wang *et al.* (2020a), The dark areas in Figure 4a represent the retained austenite whereas the lighter phase represents the ausferrite phase. As the austempering time increased, the ausferrite phase through nucleation and growth process increased as shown in Figures 4b and 4c. The ausferrite phase was in form of fine needle-like plates, these plates increased and became coarser with increasing austempering time (Figures 4a, 4b and 4c), whereas the retained austenite phase was reduced. As the austempering temperature was increased from 300 ^{o}C to 350 ^{o}C and 400 ^{o}C the acicular ferrite became coarser in structure. The ausferrite structure being more evident with 400 ^{o}C austempering time. The ausferrite phase which was in form of fine needle-like plates at 300 ^{o}C now becomes coarser and feather-like in structure at 350 ^{o}C (Figures 5a, 5b and 5c) and 400 ^{o}C, the coarsening being more evident as the austempering time is increased from 40 to 60 minutes (Figures 6a, 6b and 6c). It is evident that the morphology of acicular ferrite, the carbon content in saturated austenite and volume fraction of retained austenite are strongly dependent on the austempering temperature and austempering time. This agrees with the findings in Cui and Chen (2015) and Donnini *et al.* (2017). Also, the microstructure of the ADI samples showed higher quantity of retained austenite as the austempering temperature increased.

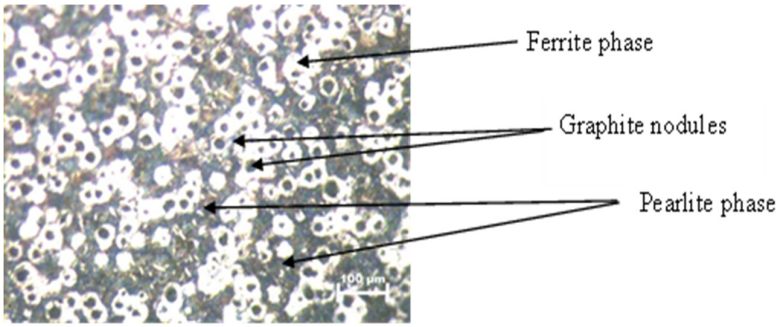

Figure 3: As cast DI sample

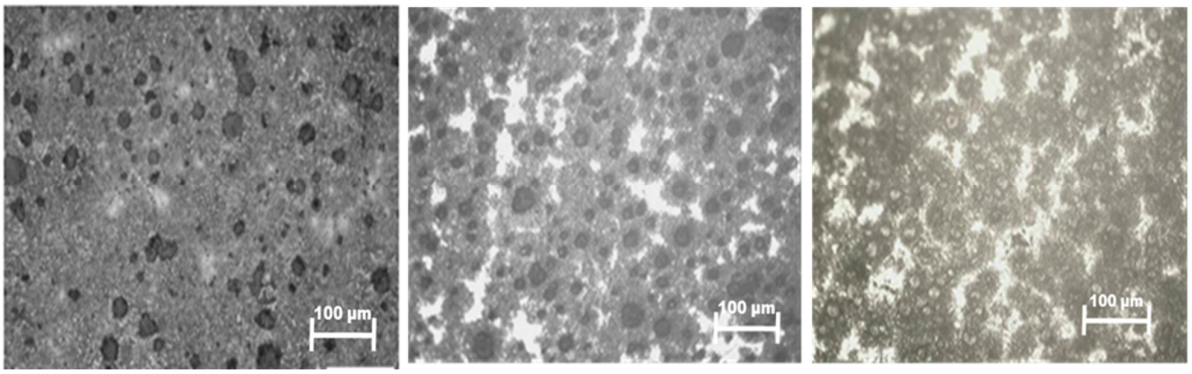

a b c

Figure 4a-c: Plate of DI austempered at 300 ºC, Holding time a) 20 mins b) 40mins c) 60 mins

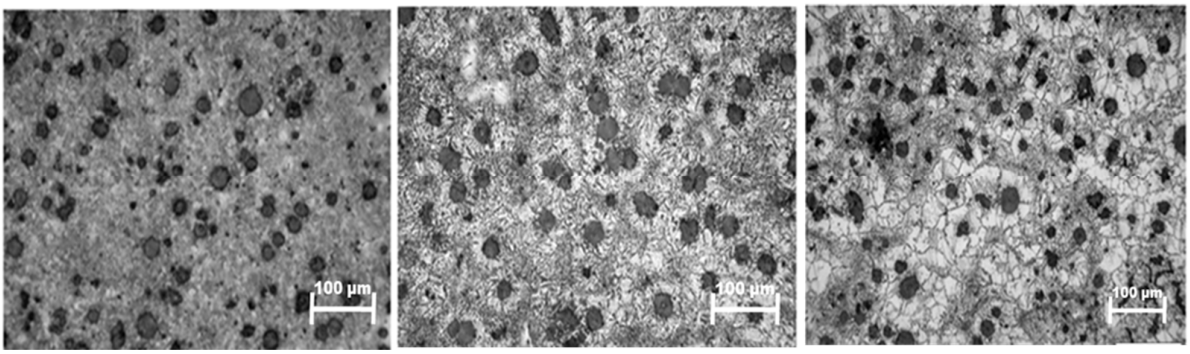

a b c

Figure 5a-c: Plate of DI austempered at 350 ºC, Holding time a) 20 mins b) 40mins c) 60 mins

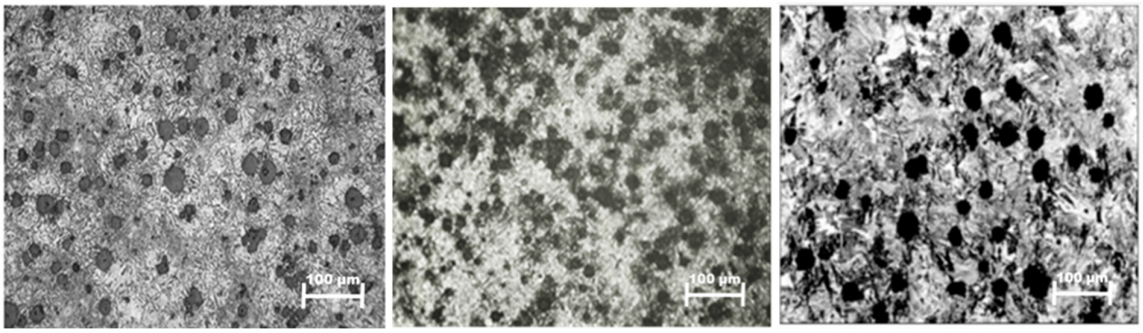

a b c

Figure 6a-c: Plate of DI austempered at 400 ºC, Holding time a) 20 mins b) 40mins c) 60 mins

3.2. Scanning Electron Micrographs of Cast and ADI Samples

The SEM micrograph and EDX analysis of the sample austempered at 300 ºC for 60 minutes is shown in Figure 7a and 7b. The coarse and feather-like structure of the acicular ferrite in the carbon enriched austenite is evident than the needle-like ausferrite structure due to the longer austempering time of 60 minutes. This is also the case for the microstructure shown in Figure 4c. The SEM micrograph and EDX analysis of the sample austempered at 350 ºC for 60 minutes is shown in Figure 8a and 8b, also that of 400 ºC for 60 minutes is shown in Figure 9a and 9b. This feather-like microstructure of the ausferrite phase is even more pronounced in Figures 8 and 9, this is attributed to the higher austempering temperatures of 350 ºC and 400 ºC, also the case in Figures 5c and 6c.

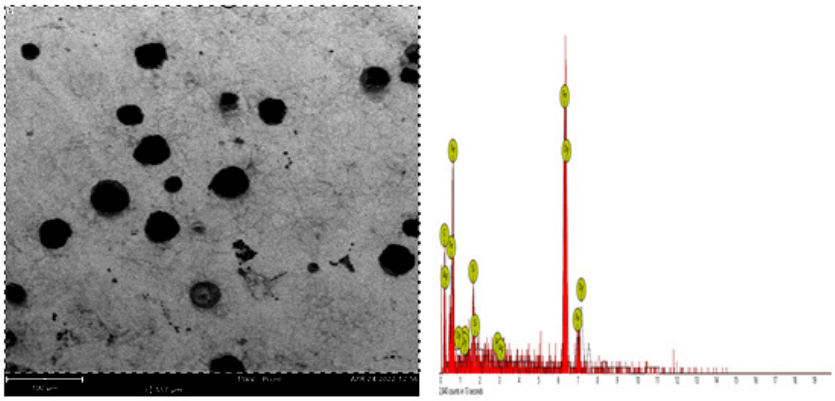

a b

Figure 7: a) SEM micrograph with b) EDX analysis for 300 ºC for 60 minutes

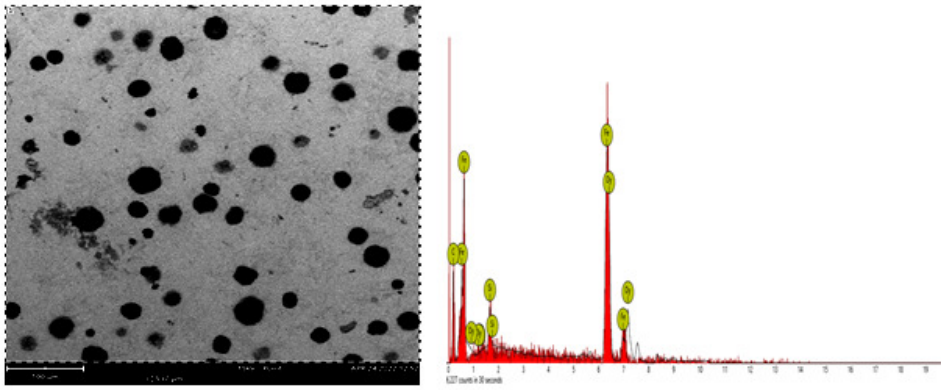

a b

Figure 8: a) SEM micrograph with b) EDX analysis for 350 ºC for 60 minutes

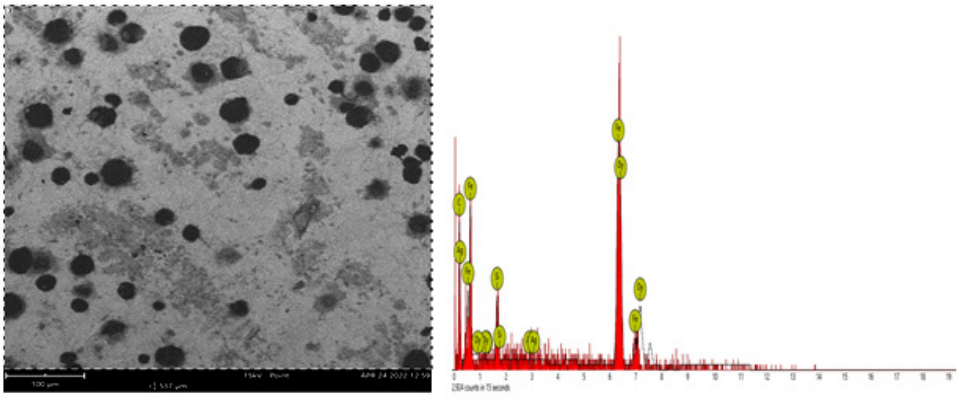

a b

Figure 9: a) SEM micrograph with b) EDX analysis for 400 ºC for 60 minutes

3.3. Mechanical Properties of As Cast and ADI Samples

3.3.1. Tensile strength

The chart for tensile strength versus austempering temperature of the as cast and austempered samples are shown in Figure 10. It is observed that the tensile strength of the samples decreased with increasing austempering temperature and soaking time. This can be attributed to increased volume of retained austenite being trapped in the microstructure as the austempering temperature is increased. The nucleation rate of acicular ferrite and austenite with high carbon content (ausferrite phase) is favoured at lower austempering temperature than the higher ones. These temperatures of 300 ^{o}C, 350 ^{o}C and 400 ^{o}C also reduced the possibility of martensite formation as these temperatures are higher than that of the martensite start temperature. As the soaking time is increased from 20 minutes to 40 and 60 minutes, growth of the ausferrite phase (acicular ferrite in carbon enriched austenite) occurred is also observed in Wang *et al.* (2020a). This growth led to the formation of coarser and feathery ausferrite structure, thereby reducing the tensile strength with increased austempering time. However, due to the increase in the amount of retained austenite at high austempering temperature a slight reduction in tensile strength was observed. For the 40 minutes-soaked sample, tensile strength values of 706, 645 and 578 MPa were observed for 300 ^{o}C, 350 ^{o}C and 400 ^{o}C austempering temperatures respectively. This trend was also observed in the study of Hegde *et al.* (2022). As shown in Figure 10, there is significant improvement of tensile strength of the ADI samples over that of the as cast structure which gave tensile strength of 480 MPa.

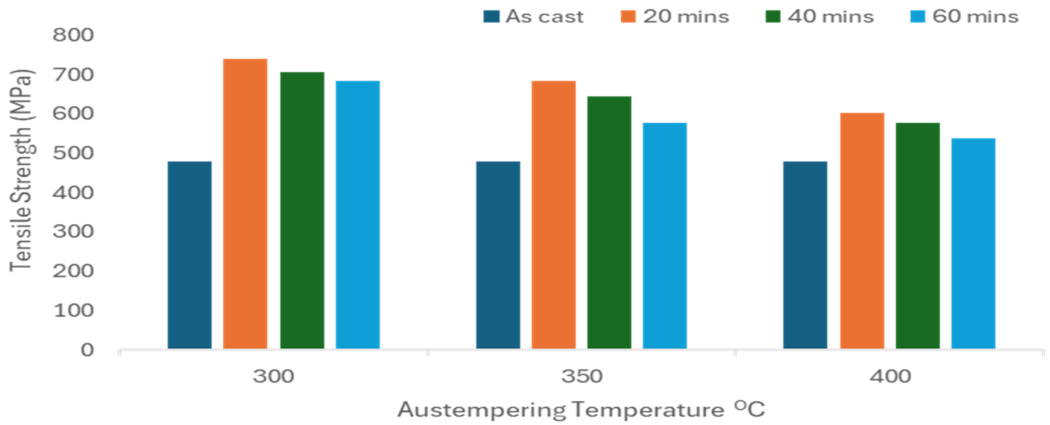

Figure 10: Chart of tensile strength versus austempering temperature for as cast and ADI samples

3.3.2. Percent elongation

The chart for percent elongation versus austempering temperature of the as cast and austempered samples are shown in Figure 11, as shown from the plot the percentage elongation increases with increase in austempering temperature and time. Austempering time showed a significant effect in the percent elongation /ductility, it was observed from Figure 11 that as the austempering time increased from 20, 40 to 60 minutes for each austempering temperature the percent elongation increased, this greater ductility obtained at higher soaking time results from the growth of the nucleated ausferrite phase from needle-like shape to the coarser and feathery ausferrite structure. At higher austempering temperatures there is more retained austenite than occurs at lower austempering of 300 ^{o}C (Figures 4 - 6), this accounts for the higher ductility of 4.1 and 5.7% elongation at 350 and 400 ^{o}C austempering temperatures respectively for samples austempered for 20 minutes, this trend was also observed for 40- and 60-minutes austempering times. Also, greater ductility is obtained for a more coarser and feathery ausferrite structure (Figures 4-6). The temperature of 300 ^{o}C favours the nucleation of the ausferrite

phase as there is larger supercooling, this larger supercooling favours formation and reduction of critical radius of the nucleating phase i.e. ausferrite phase. This trend is in consonance with that observed by the researchers in Hegde *et al.* (2022). At austempering temperature of 400 °C improved ductility is observed with compromise on tensile strength, whereas the opposite in the case at 300 °C.

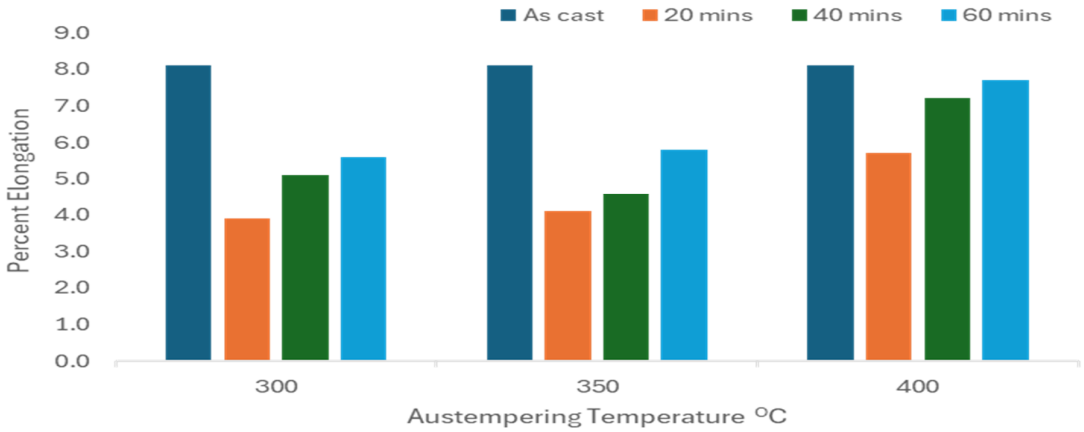

Figure 11: Chart for percent elongation versus austempering temperature for as cast and ADI samples

3.3.3. Hardness

The chart for vickers hardness value versus austempering temperature of the as cast and austempered samples are shown in Figure 12, as shown the plot shows that hardness decreases with increase in austempering temperature and time. There is significant improvement over the as cast hardness value of 390 Hv in all the austempered samples. The increase in the amount of retained austenite at higher austempering temperatures of 350 and 400 °C caused the reduction in hardness values, nucleation of the ausferrite phase occurred more at lowest temperature of 300°C due to greater supercooling consequently increasing hardness of those samples. This trend was also observed in related studies conducted by Hsu and Lin (2011) and Wang *et al.* (2016), these researchers concluded that the hardness and tensile strength of single-step ADIs decreased, and ductility increased with increasing austempering temperature or holding time. This could be attributed to more unstable austenite transformation into ausferrite structure with high carbon content during the isothermal heat treatment process, and less martensite formation in the final ADI matrix.

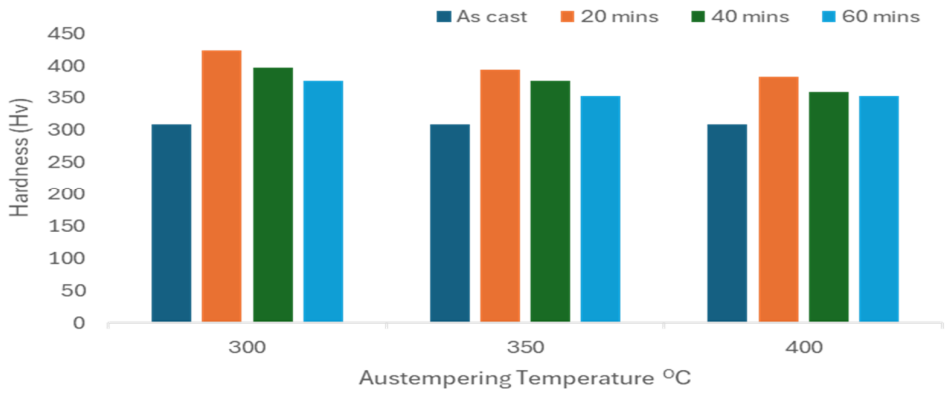

Figure 12: Chart for vickers hardness versus austempering temperature for as cast and ADI samples

3.4. Wear rate

The chart of the wear rate versus austempering temperature of the as cast and austempered samples are shown in Figure 13. The plot shows that wear rate increases with increase in austempering temperature and time, from Figure 13, wear rate increases with an increase in the austempering temperature. At the lowest austempering temperature of 300 ºC, wear rate is low (0.47 mm^3/s), this is attributable to the finer lower ausferritic structure with high hardness value 424 Hv (for samples austempered for 20 minutes). At elevated austempering temperatures of 350 ºC and 400 ºC, wear rate is higher: 0.7 and 0.94 mm^3/s respectively due to the presence of coarse upper ausferrite. Also the increased wear rate at higher temperatures of 350 ºC and 400 ºC, could also be attributed to the greater amount of retained austenite which is a softer phase in comparison with the ausferrite phase. The wear rate of as-cast samples is significantly higher than austempered samples, because of the softer ferritic and pearlitic structure. Also, the wear rate increases with increased austempering time due to growth of the ausferrite structure from its formation with finer nucleated structure to the coarser structure which occurs with increase in austempering time. These findings are in agreement with studies conducted in Sellamuthu *et al.* (2018) and Sahin and Durak (2017). These researchers observed that increasing the austempering temperatures and holding duration could result in significantly high wear loss on single-step ADI specimens in rotational ball-on-disk sliding tests. It is observed that the wear rate increased with decrease in the hardness of the ADI samples, showing a indirect correlation between wear rate and hardness of the ADI samples.

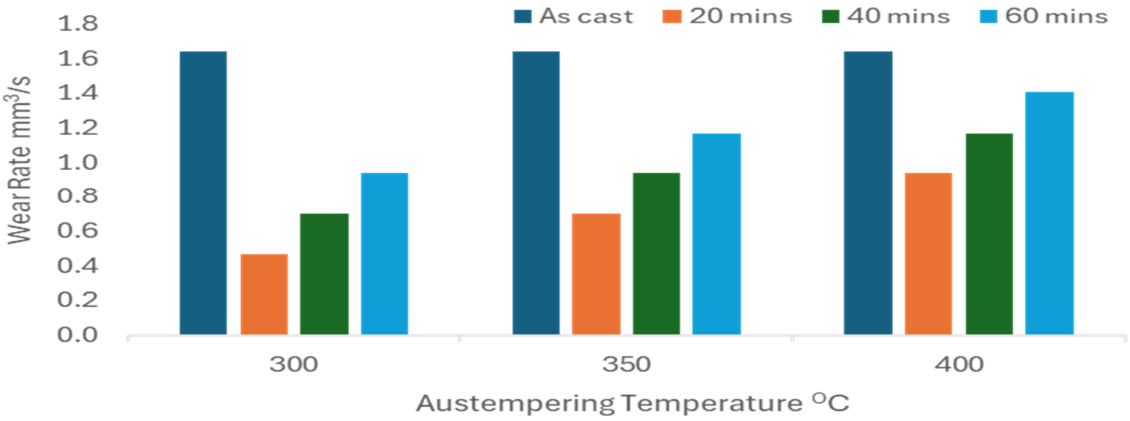

Figure 13: Chart for wear rate versus austempering temperature for as cast and ADI samples

3.5. X-Ray Diffraction (XRD)

The XRD patterns conducted for the control sample (which was not austempered), the sample austempered at 300, 350 and 400 ºC (with holding time of 40 minutes) are shown in Figure 14, . The XRD results confirmed that the main phases present in the samples were austenite (γ) and ferrite (α) phases. For the control sample (as cast), a sharp peak is observed at 2θ bragg's angle of about 45º corresponding to α ferrite phase occurring at (110) plane, other peaks indicative of Fe_3C were also observed close to the α ferrite peak suggesting the presence of the pearlite phase. At temperature of 300 ºC, the α Fe BCC lattice peak occuring at (110) plane and γ FCC phase occuring at (111) and (002) plane corresponding to 2θ of about 42º and 50º respectively were observed close to each other suggesting the formation of the ausferrite phase. At 350 ºC, greater intensity of these peaks were observed. At 400 ºC, additional α ferrite peak occuring at bragg's angle of 65º on (200) plane was observed. This can be attributed to the growth of the nucleated ausferrite phase. The XRD plot validated the fact that as temperature increased, the ausferrite phase became more stabilized. This is in consonance with the studies conducted by Sellamuthu *et al.* (2018) and Regita *et al.* (2021).

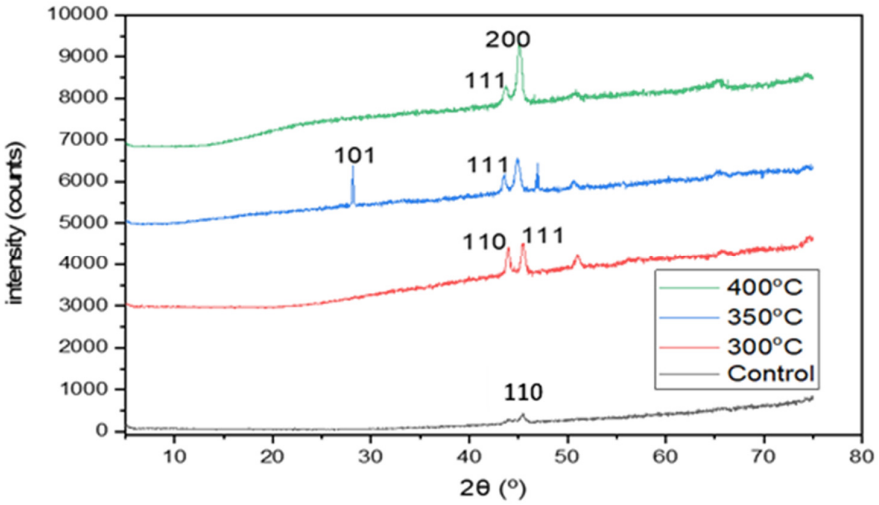

Figure 14: XRD pattern for control, 300 °C, 350 °C and 400 °C (40 minutes austempering time) samples

4. CONCLUSION

In this study, green sand mould cast DI which consisted of graphite nodules in pearlitic ferritic matrix was subjected to varying austempering heat treatment parameters: temperature and time to determine their effect on mechanical and wear properties of the resulting ADI samples. Varying temperatures of 300 °C, 350 °C and 400 °C and varying times of 20, 40 and 60 minutes were adopted. Microstructures of all austempered samples at the various austempering temperature and times adopted consisted of various proportions of acicular ferrite and carbon-enriched austenite, called ausferrite, graphite nodules and retained austenite phase. The results of these study have shown that these two parameters significantly influence microstructural evolution and consequently the mechanical and wear rates of the ADI samples. The tensile strength and vickers hardness values decreased with increase in austempering temperature and time whereas the ductility (percent elongation) and wear rates increased with increase in austempering temperature and time.

5. ACKNOWLEDGMENT

The authors wish to acknowledge the assistance of the laboratory staff of Department of Metallurgical and Materials Engineering Laboratory of the University of Lagos. Also, the staff at the Foundry in Nigerian Machine Tools Osogbo, Osun state, for their contribution in sample preparation.

6. CONFLICT OF INTEREST

There is no conflict of interest associated with this work.

REFERENCES

ASTM A 536. (1998) Ductile iron casting specific: tensile–yield– elongation. *Annual Book of ASTM Standard*, American Society for Testing and Materials International, West Conshohocken, PA.

ASTM E3-11. (2011) Standard Guide for Preparation of Metallographic Specimens[S]. *Annual Book of ASTM Standards,* American Society for Testing and Materials International, West Conshohocken, PA.

ASTM E8/E8M. (2022) Standard Test Methods of Tension Testing of Metallic Materials, *Annual Book of ASTM Standard*, American Society for Testing and Materials International, West Conshohocken, PA.

ASTM E384-11. Standard Test Method for Knoop and Vickers Hardness of Materials. *Annual Book of ASTM Standard*, American Society for Testing and Materials International, West Conshohocken. PA.

ASTM G99. (2017) Standard Test Method for Wear Testing with a Pin-on-Disk Apparatus. *Annual Book of ASTM Standard*, American Society for Testing and Materials International, West Conshohocken. PA.

ASTM E2349. (2019) Standard Practice for Safety Requirements in Metal Casting Operations: Sand Preparation, Molding, and Core Making; Melting and Pouring; and Cleaning and Finishing *Annual Book of ASTM Standard*, American Society for Testing and Materials International, West Conshohocken. PA.

Bialobrzeski, A. and Pezda, J. (2014). Testing of heating and cooling process of ADI cast iron with use of ATND method. *Archives of Foundry Engineers*, 8, pp. 11–4.

Chiniforush, E. A., Rahimi, M. A. and Yazdani, S. (2016). Dry sliding wear of Ni alloyed austempered ductile iron. *China Foundry*, 13(5), pp. 361–367..

Cui, J. and Chen, L. (2015). Microstructures and mechanical properties of a wear-resistant alloyed ductile iron austempered at various temperatures. *Metallurgical Material Transaction,* 46A, pp. 3627–34.

Donnini, R., Fabrizi, A., Bonollo, F., Zanardi, F. andAngella, G. (2017). Assessment of the microstructure evolution of an austempered ductile iron during austempering process through strain hardening analysis. *Metallurgical Materials International*, 23(5), pp. 855–64.

Hegde, A., and Sharma, S. (2018). Comparison of machinability of manganese alloyed austempered ductile iron produced using conventional and two step austempering processes. *Materials Research Express*, *5*(5), pp. 056519.

Hegde, A., Sharma, S., Hande, R., B M, G. and Jones, I. P. (2022). Microstructure and mechanical properties of manganese-alloyed austempered ductile iron produced by novel modified austempering process. *Cogent Engineering*, *9*(1), pp. 1-11.

Hsu, C. and Lin, K. (2011). A study on microstructure and toughness of copper alloyed and austempered ductile irons. *Material Science Engineering,* 528(18), pp. 5706–12.

Krawiec, H., Lelito, J., Mróz, M. and Radon, M. (2023). Influence of heat treatment parameters of austempered ductile iron on the microstructure, corrosion and tribological properties. *Materials*, 16(11), pp. 4107.

Laino, S., Sikora, J. A. and Dommarco, R.C. (2008). Development of wear resistant carbidic austempered ductile iron (CADI). *Wear*, 265, pp. 1–7.

Magalhães, L., Martins, R. and Seabra, J. (2012). Low loss austempered ductile iron gears: Experimental evaluation comparing materials and lubricants. *Tribology International,* 46, pp. 97-105.

Mandal, S., Maity, A. (2013). Austempered ductile iron material for the design of agriculture machinery. *Mechanical Engineering*. 60, pp. 16140–5.

Mussa, A., Krakhmalev, P. and Bergström, J. (2022). Wear mechanisms and wear resistance of austempered ductile iron in reciprocal sliding contact. *Wear*, 498–499(7), pp. 204305.

Olivera, E., Jovanovic, M., Sidanin, L., Rajnovic, D. and Zec, S. (2006). The austempering study of alloyed ductile iron. *Materials and Design*, 27, pp. 617-622.

Regita, B., Antanas, C., Ramunas, C., Audrius, J., Aliaksandr, B., Dzianis, M., Aleh, N., Liudmila, S., Sergei, S. (2021). Influence of austempering temperatures on the microstructure and mechanical properties of austempered ductile cast iron. *Metals,* 11(6), pp. 967.

Sahin, Y. and Durak, O. (2017). Abrasive wear behavior of austempered ductile iron. *Materials and Design,* 28, pp. 1844–50.

Sellamuthu, P., Samuel, D., Dinakaran, D., Premkumar, V., Li, Z. Seetharaman, S. (2018). Austempered ductile iron (ADI): Influence of austempering temperature on microstructure, mechanical and wear properties and energy consumption. *Metals,* 8(1), pp. 53.

Rajan, T. V., Sharma, A. K. and Sharma, C. P. (2011). Heat treatment principles and techniques. PHI Learning, 2 ed. ISBN, 8120340957 New Delhi.

Šolić, S., Godec, M., Schauperl, Z. and Donik, Č. (2016). Improvement in abrasion wear resistance and microstructural changes with deep cryogenic treatment of austempered ductile cast iron (ADI). *Metallurgical and Materials Transactions A: Physical Metallurgy and Materials Science*, 47(10), pp. 5058–5070.

Upkar, Nausad K., Rone. and Akhilesh P. T. (2019). Paper on the effect of copper on austempering behavior of ductile Iron: A Review. *International Journal of Engineering Research in Mechanical and Civil Engineering*, 4(9). pp. 1-7.

Vidyarthee, G. and Singh, K. (2014). Thin wall austempered ductile iron: a best replaceable material to steel and aluminum. *International Journal Mechanical Engineering and Robotics Research,* 3(3), pp. 465–73.

Wang, B., Barber, G. C., Qiu, F., Zou, Q. and Yang, H. (2020a). A review: phase transformation and wear mechanisms of single-step and dual-step austempered ductile irons. *Journal of Materials Research and Technology*, *9*(1), pp. 1054–1069.

Wang, B., Qiu, F., Barber, G. C, Pan, Y., Cui, W. and Wang, R. (2020b) Microstructure, wear behavior and surface hardening of austempered ductile iron. *Journal of Materials Research and Technology*, *9*(5), pp. 9838–9855.

Wang, B., Barber, G., He, M., Sun, X., Shaw, M., Slattery, B. and Seaton, P. (2016). Study of ausferrite transformation kinetics for austempered ductile irons with and without Ni. *SAE Technical Paper.* World Congress Exhibition.

Yang, J. and Putatunda, S. K. (2005). Effect of microstructure on abrasion wear behavior of austempered ductile cast iron (ADI) processed by a novel two-step austempering process. *Material Science Engineering A*, 406, pp. 217–28.

Zhou. R., Jiang, Y., Lu, D., Zhou, R. and Li, Z. (2001). Development and characterization of a wear resistant bainite/martensite ductile iron by combination of alloying and a controlled cooling heat-treatment. *Wear,* 250, pp. 529–34.